

# Reconstructing 3D Structure from Amazon Product Images

Jason van der Merwe  
jasonvdm@stanford.edu

Andrew Giel  
agiel@stanford.edu

Bridge Eimon  
beimon@stanford.edu

CS 231A Stanford University  
December 8, 2013

---

## Abstract

This paper presents the methods we explored for three dimensional structural reconstruction from two dimensional product images on Amazon.com. We began with our own images of a volleyball for a proof of concept. Using SURF and RANSAC, we found correspondence points among the images. After we retrieved these points, we computed structure from motion (SfM) among image pairs. To stitch the SfMs from image pairs together, we used RANSAC and the SURF descriptors for the points in the 3D point cloud to combine the point clouds from each image pair together. After this step, we were able to plot the 3D structure. Our method produced accurate results for the volleyball images, however, we were unable to successfully plot the structures for Amazon products for a variety of reasons. One obstacle is that Amazon product images are taken with a large amount of rotation between each image, so the amount of redundancy is low. Additionally, most products exhibit considerable symmetry, so the performance struggles from SURF and RANSAC. Our paper further analyzes the issues we encountered and the steps that Amazon could take in order to ensure their product images could be used for 3D reconstruction.

## 1. Introduction

This project, reconstructing 3D models from Amazon product images, is the first step of a larger goal to build a database of 3D objects by crawling the web. This database can then be used to assist in many other object detection tasks, such as identifying objects in your home or from a cell phone camera. One important component of making such a system is to build 3D object models from multiple views of web images. SfM is generally performed using a number of images carefully taken of the same object. Can we use SfM from product images taken by different users? Amazon often has a collection of images for each object uploaded by differ-

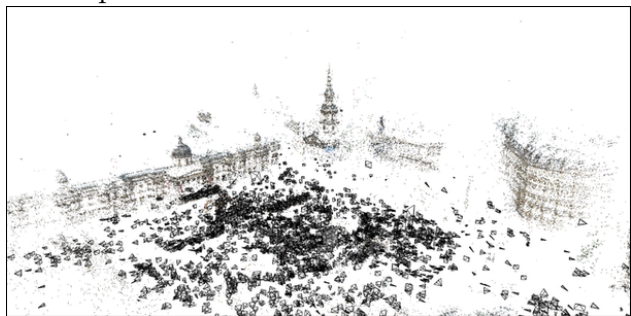
ent users. These views were all taken with different cameras in different lighting / backgrounds, which adds a challenge. Can we combine these images to create 3D object models?

### 2.1 Previous Work

Recreating the structure of an object from a set of images has been explored by many instances of previous research, even in a completely unsupervised and automatic fashion.

In fact, the concept of taking images available online of the same object or scene and then reconstructing the three dimensional properties from these images has been achieved by previous research. In a paper

entitled ‘Photo Tourism: Exploring Photo Collections in 3D’, Noah Snavely presents a system that retrieves images of famous landmarks and then infers the structure of the landmarks in three dimensions as well as the pose and location of the cameras which captured the images. After establishing correspondences, Navelly utilized the Levenberg-Marquardt algorithm to solve the least-squares problem of sparse bundle adjustment. Once this structure known, Snavely and his team were able to rerender the scene as well as the position of the cameras.



A key portion of the reconstruction process, as mentioned above, is establishing correspondences between the images. This can be achieved via expensive manual annotation or by solving the longstanding correspondence problem. David Lowe’s work on the Scale-Invariant Feature Transform (SIFT) helped to address this cardinal problem in the vision community. By implementing a difference-of-Gaussian function to identify points of interest in the images, Lowe was able to then localize and establish their dominant orientation. Once the keypoints were defined and descriptors established, Lowe utilized best-bin-first search in order to find the best match from any one keypoint of an image to a keypoint from another image, using Euclidean distance as the ranking metric. In order to determine the probability of a match, Lowe used the ratio of the distance to the best match to the distance of the second best

match, eliminating matches with a distance ratio over a certain threshold. Combining this methodology with a model-generating procedure such as Random Sample Consensus (RANSAC) has proven to be effective in estimating the correspondence problem, and was utilized in our implementation as well.

Given a set of correspondences, recovering the structure from motion is a non-trivial problem. Tomasi and Kanade, in their seminal paper, present a method for extracting scene geometry and camera motion from a matrix  $W$  derived from the measurements and correspondences. Tomasi and Kanade realized that the points are represented within a low-dimension subspace of  $W$ , allowing them to be extracted via Singular Value Decomposition. This method performs best when used on points without occlusions, yet methods are presented to extrapolate measurements.

In 2005, Lowe published a paper titled ‘Unsupervised 3D Object Recognition and Reconstruction in Unordered Datasets’ in which he outlined a procedure to recreate the 3D structure of objects using his SIFT feature descriptors, RANSAC, and sparse bundle adjustment without any user input. He proved that such a process was possible, giving a technical foundation for our experiments with Amazon.

## 2.2 Advancements

Our experiments take the concepts presented by the Snavely Photo Tourism paper and Lowe’s unsupervised reconstruction paper and test the limits to which these concepts can be applied, by attempting to reconstruct products on Amazon. Product photos on Amazon present a number of challenges which make the reconstruction process difficult, which is elaborated in the Error Analysis section. Testing methods presented in

these papers on imperfect, noisy, and occluded data helps to define the limits of our ability to successfully recreate three dimensional structure. Additionally, by attempting to apply this sort of technique to a new domain and create a new product for Amazon we can make a commercial impact and not just an academic or theoretical assessment.

### 3.1 Technical Summary

We implemented our system incrementally, starting first by testing our reconstruction on manually annotated correspondences with images we took ourselves in a controlled environment. Our SfM is computed using the Tomasi-Kanade factorization algorithm. This allowed us to have a full measurement matrix for our Tomasi-Kanade. Once this was verified to work on with manually annotated images of our own we implemented automatic correspondence using SIFT, SURF, and ORB descriptors, matching using Euclidean distance and verifying by comparison to the second closest match. In order to refine our correspondence matches we used RANSAC, experimenting with different thresholds. In the case where we have multiple point clouds (SfMs) corresponding to structures inferred from a pair of two images, we combined these point clouds using a similar procedure. Given a set of points in three dimensions and their corresponding descriptors (SIFT, SURF, ORB), we determined the best match between these clouds via RANSAC. Using RANSAC on the three dimensional points, we generate a three dimensional homography. This homography can be used to translate the points in one point cloud to the points in another point cloud, merging the structures captured. Once we tuned our system to work on our own images, we tested on Amazon images.

Our method can be broken down into 4 discrete steps: description, matching, inference of structure, and merging of structures.

### 3.2 Description

In order to obtain keypoints and descriptors from images, we tried SIFT, SURF and ORB. After experimenting, we found that SURF obtained the most keypoints and descriptors for our images. We utilized the OpenCV implementations of these algorithms. These functions returned a 128-dimension descriptor vector for every keypoint in the image plane. These keypoints and descriptors were then passed to our matching algorithms.

### 3.3 Matching

To match points, we calculated initial matching of our keypoint descriptions using the Fast Library for Approximate Nearest Neighbors (FLANN). We chose this algorithm because it uses a k-d tree structure which reduces the nearest neighbors calculation to run in  $O(\log N)$  time, a drastic speed improvement. We only keep keypoint pairs where the ratio of the nearest neighbor and the second nearest neighbor is less than 0.7 as presented in Lowe's paper. This enables us to remove matches where we are not confident in our match. Once we have this set of matches, we performed Random Sample Consensus (RANSAC) to remove any outlier point pairs that do not fit a homography projecting keypoints from the first image into the second. The way we do this is to:

- 1) Select 4 random keypoints from the first image. We pick four keypoints, because this is the minimum number of points needed to calculate a homography between 2D images
- 2) We compute a homography  $H$  which maps

our 4 random keypoints from image 1 into image 2. We calculated this homography  $H = X'X^{-1}$  where

$$X' = \begin{bmatrix} Kp_{2,1,x} & Kp_{2,2,x} & Kp_{2,3,x} & Kp_{2,4,x} \\ Kp_{2,1,y} & Kp_{2,2,y} & Kp_{2,3,y} & Kp_{2,4,y} \\ 1 & 1 & 1 & 1 \end{bmatrix}$$

$$X = \begin{bmatrix} Kp_{1,1,x} & Kp_{1,2,x} & Kp_{1,3,x} & Kp_{1,4,x} \\ Kp_{1,1,y} & Kp_{1,2,y} & Kp_{1,3,y} & Kp_{1,4,y} \\ 1 & 1 & 1 & 1 \end{bmatrix}$$

3) Calculate how many keypoint correspondences are within a tolerance error and store these inliers.

4) Repeat 1-3 for a predetermined amount of iterations (we used 1000) to find the model that keeps the most inliers. We then returned the inliers and the model.

Once we have done this, we have a set of geometrically consistent matches to use in computing the structure of the object.

### 3.4 Structure

Once we have obtained this set of consistent matches, we want to obtain the structure in a point cloud via the Tomasi-Kanade algorithm.

The first step in this process is to center the image points. This is achieved by subtracting the centroid of the points from each of the points. More formally, for every point  $x_{ij}$  on camera  $i$  we subtract  $\bar{x}_i$ .

$$\hat{x}_{ij} = x_{ij} - \bar{x}_i$$

$$\hat{x}_{ij} = x_{ij} - \frac{1}{n} \sum_{k=1}^n x_{ik}$$

Where  $n$  is the number of points on one image. Note that this can be expressed equiv-

lently as a function of the camera in the affine model.

$$x_{ij} = A_i X_k + b_i$$

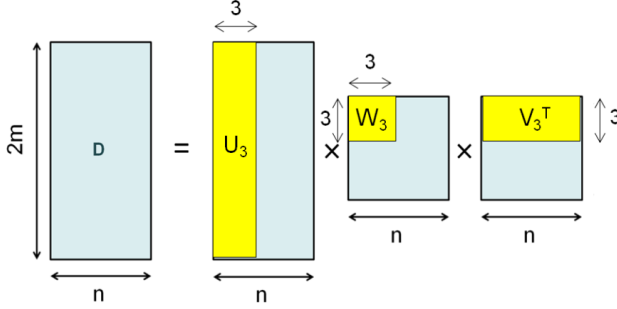
$$\hat{x}_{ij} = A_i X_j + b_i - \frac{1}{n} \sum_{k=1}^n (A_i X_k + b_i)$$

$$\hat{x}_{ij} = A_i (X_j - \frac{1}{n} \sum_{k=1}^n X_k)$$

This means that every point  $\hat{x}_{ij} = A_i \hat{X}_j$ , which means that if we put the center of the world coordinate system as the centroid,  $\hat{x}_{ij} = A_i \hat{X}_j = A_i X_j$ , allowing for factorization to occur.

With our newly centered data we can perform the factorization that is the key insight of the Tomasi-Kanade algorithm. First, it is necessary to create a measurement matrix  $D$  of size  $(2m \times n)$ , where  $m$  is the number of frames and  $n$  is again the number of points. The reason the factor of two is present is that the first  $m$  dimensions of the matrix are the  $x$  coordinates of the points in the image plane, while the remaining  $m$  dimensions are the  $y$  coordinates.

With our measurement matrix  $D$ , we know both the structure and motion are obtainable via factorization. The measurements  $D$  can be broken into  $MS$ , where  $M$  is the motion (camera matrices and orientations) of size  $(2m \times 3)$  and  $S$  is the structure matrix (3 dimensional points  $X_j$ ) of size  $(3 \times n)$ . We cannot determine  $MS$  by a simple factorization, but we can perform Singular Value Decomposition (SVD) to have access to the component matrices,  $D = U W V^T$ . We can recover  $MS$  by taking portions of the SVD components.  $M = U_3$ , or the first 3 columns of  $U$ . Similarly,  $S = W_3 V_3^T$  or the first 3 columns of the the first three rows of  $W$  and the first 3 dimensions of  $V^T$ . The resulting  $S$ , of size  $(3 \times n)$ , is a column matrix of the points, our intended result.



### 3.5 Merging Structures

Once we computed our multiple point clouds using SfM, the last step was to aggregate all the points into one output space. In order to do this, we used a modified version of RANSAC applied to the points in 3D space in our point clouds. To merge two point clouds together, we used the SURF descriptors of the image common to both point clouds to find the matches between points in the point clouds. The next step is to use RANSAC to find a 4x4 homography which maps points from the first point cloud to the second with the largest number of inliers.  $H$  is a homogenized 4x4 matrix, so we homogenized the first point cloud, the calculated the points from the first cloud into the output space of the second point cloud by  $P_2 = H \times \text{homogenized}P_1$ . Once we then dehomogenized these points, we added them into the output space of the second point cloud, resulting in an image containing an aggregation of both point clouds. We then take two of these combined set of point clouds and combine them as well until we have a single point cloud containing all our keypoints.

### 4.1 Experiments Summary

We tested our implementation on many different sets of images. This includes images we took ourself, images taken from Amazon, different objects, different resolutions, and image sets with different degrees of rotation

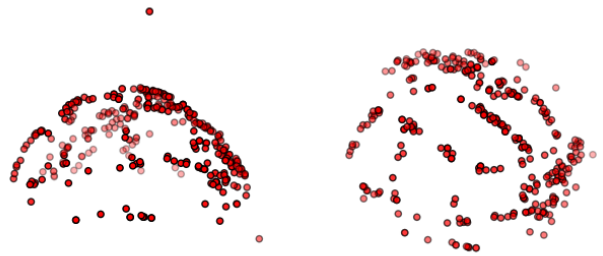
between individual images. Listed here are some of the characteristics of the images on Amazon that affected our implementation's performance in the reconstruction process.

### 4.2 Comparison of Descriptors

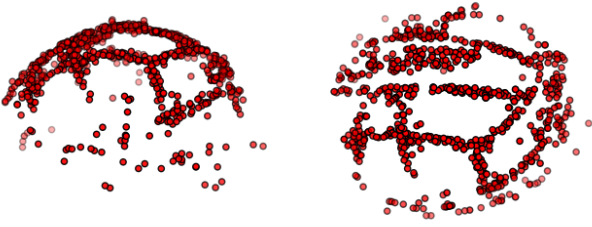
As explained earlier, our implementation experimented with multiple different types of descriptors- namely SIFT, SURF, and ORB. We found that in order to create a point cloud that was representative of the structure of the object we wanted to maximize both the number of keypoints detected and the number of matches determined by our previously mentioned method (3.2). In the end, we chose SURF as our primary descriptor as this method maximized these metrics. The table below outlines the differences in the descriptors on one of our own images of a volleyball we used for testing.

Method	NumKeypoints	NumMatches
SURF	2712	248
SIFT	1180	144
ORB	500	19

Also seen here are the recovered structures from each of the descriptor methods used. Note there is no structure retrieved using ORB, as it did not output a sufficient number of correspondences.



A volleyball reconstructed using SIFT shown from two angles.

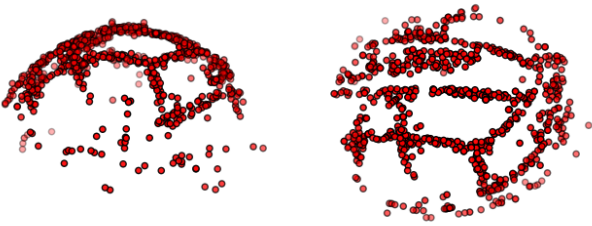


A volleyball reconstructed using SURF shown from two angles.

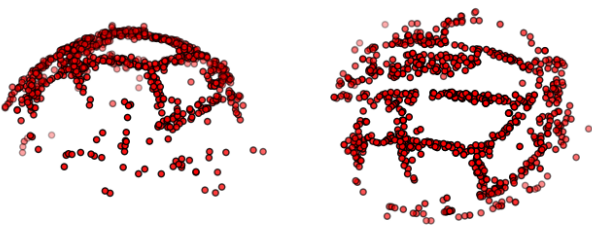
It is clear that SURF is clearly more robust and produces far better results.

### 4.3 Different Image Resolutions

On a related note, we found the resolution of the image drastically affected our reconstruction due to the number of keypoints identified. As would be expected, larger images (those with higher resolution) resulted in more keypoints than smaller images. More keypoints allows for more potential matches, meaning a larger pointcloud and a more defined reconstruction. Lower resolution images, like many of those found on Amazon, resulted in worse constructions.



Structure inferred from large images ( $2000 \times 1325$ )

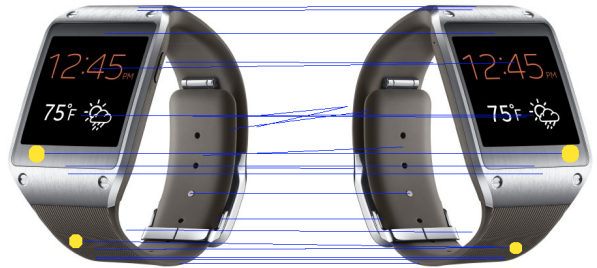
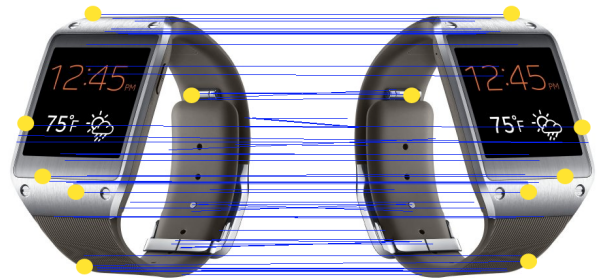


Structure inferred from smaller images ( $755 \times 500$ )

It should be noted that the smaller image here is representative of the median of images found on Amazon, with many images having much worse resolution.

### 4.4 Symmetry in Objects

One of the largest problems we faced on the Amazon product images was the remarkable amount of symmetry in these images intended for advertisement. Often these images depicted symmetric objects with glares and reflections that were mirrored between the two images. This exposed a fundamental flaw or weakness in our matching process, as opposite sides of a symmetric object which appear identical would be matched. This led to enormous reconstruction error that resulted in nonsense structural point clouds. Our best example of this occurs in a pair of images of a smartwatch, where the left side of the watch in one image mirrors the right side of the paired image. The two below images are of the matches generated before and after RANSAC, with yellow indicating areas where this problem of symmetry occur.



There are clear problems with symmetry in both cases. RANSAC removes many of the matches that are incorrect due to symmetry, however, a few incorrect matches slip through RANSAC. There were so few matches after RANSAC that it was impossible to plot the

structure of the watch with any degree of accuracy. Unfortunately, this problem occurs with many products.

## **4.5 Angular Disparity**